Journal of Thermal Analysis and Calorimetry (2023) 148:4641–4649
https://doi.org/10.1007/s10973-023-11942-7

Instrumental investigations of promestriene: first report regarding the solid-state characterization and compatibility with pharmaceutical excipients

Cosmina Bengescu[1] · Adriana Ledeți[2] · Tudor Olariu[2] · Denisa Cîrcioban[2] · Cornelia Muntean[1] · Gabriela Vlase[3] · Titus Vlase[3] · Carmen Tomoroga[2] · Anca Octavia Dragomirescu[2] · Daniela Dascălu[4] · Lenuța-Maria Șuta[2] · Ionuț Ledeți[1,2] · Marius Murariu[2,5]

Received: 25 January 2022 / Accepted: 1 January 2023 / Published online: 19 January 2023

Abstract

In this paper, ten samples containing promestriene (PRMS) were investigated, namely the pure active pharmaceutical ingredient (API) and nine binary mixtures prepared with commonly used excipients in solid pharmaceutical formulations. The necessity of such study is represented by the fact that the physicochemical screening of PRMS is not reported in the literature. Also, as convergent arguments for the necessity of this study, it can be mentioned that on Romanian pharmaceutical market, promestriene containing formulations are no longer commercialized since 2015, creating health problems to a large category of patients. As such, this study can serve as a starting point for the adequate selection of ingredients used in magistral preparations, with increased stability and bioavailability. The study revealed that PRMS is compatible with all of the selected excipients, namely methyl 2-hydroxyethyl cellulose (tylose), methyl cellulose (MethocelTM), starch, mannitol, magnesium stearate, magnesium citrate, Talc, colloidal SiO_2 (aerosil) and polyvinylpyrrolidone K-30 (PVPK30), as confirmed by universal attenuated total reflectance Fourier transform infrared (UATR-FTIR) spectroscopy, powder X-ray diffraction patterns and thermal analysis.

Keywords Promestriene · Excipient · Compatibility study · Preformulation · Physicochemical behavior

Introduction

Promestriene (3-Propoxy-17β-methoxy-1,3,5(10)-estratriene; abbreviated PRMS) is a synthetic estrogen analog of estradiol, that has been reported to significantly improve the symptoms of vaginal atrophy and urogenital disorders caused by estrogen deprivation [1, 2].

PRMS has been studied and used in Europe, Asia and South America to treat symptoms such as tissue thinning and shrinking, vaginal dryness, soreness, painful intercourse and urinary incontinence [2]. Furthermore, it is been shown to be effective in reversing atrophic changes caused by estrogen deficiency in women undergoing natural or surgically induced menopause [1].

The use of vaginal estrogens is controversial in gynecological oncology patients as they are more likely to develop severe vaginal atrophic symptoms. Thus, they need it more frequently, but, at the same time, most of them have an estrogen-sensitive neoplasm and fear its possible systemic effect. The safety data available is assuring that PRMS can be used

✉ Cornelia Muntean
cornelia.muntean@upt.ro

1 Faculty of Industrial Chemistry and Environmental Engineering, Politehnica University of Timișoara, Vasile Parvan Street 6, 300223 Timisoara, Romania

2 Faculty of Pharmacy, Advanced Instrumental Screening Center, University of Medicine and Pharmacy "Victor Babeş", Eftimie Murgu Square 2, 300041 Timisoara, Romania

3 Research Centre for Thermal Analysis in Environmental Problems, West University of Timisoara, Pestalozzi Street 16, 300115 Timisoara, Romania

4 Faculty of Chemistry, Biology, Geography, West University of Timisoara, Pestalozzi Street 16, 300115 Timisoara, Romania

5 Faculty of Medicine, University of Medicine and Pharmacy "Victor Babeş", Eftimie Murgu Square 2, 300041 Timisoara, Romania

in a proper way and in selected cases to treat vaginal atrophy even in patients with cancer [1, 3]. The chemical structure of PRMS is presented in Fig. 1.

PRMS was initially studied and developed by Monaco Dudley, and the US patent approval was obtained in 1977. Colpotrophine ® entered the French market in 1975, and the formulation consisted in vaginal capsules or cream containing PRMS [4]. Later, vaginal tablets containing PRMS and chloroquinaldol (CQA) were developed [5]. Martindale Drug Manual has entered the PRMS + CQA tablet formulation onto the pharmaceutical market in more than 40 countries, for over 40 years [4]. More recently, in 2019, Chen X. and Guo H. published a comparative study regarding the effects of PRMS + CQA vaginal tablets and suppositories on serum inflammatory factors and immune function in patients with chronic cervicitis and Human Papilloma Virus (HPV) infection [5], leading to the conclusion that the tablet formulation is more effective in comparison with suppositories.

PRMS is one of the least studied estrogens, since Web of Science of Clarivate Analytics® indexes up to October 2022 solely 34 scientific papers [6], none of them being related to preformulation studies for this active pharmaceutical ingredient, which was commercialized on Romanian pharmaceutical market as vaginal capsules up to June 2015. Since then, the holder has withdrawn the marketing authorization for this drug due to commercial reasons, and no other equivalent formulation was authorized on the Romanian pharmaceutical market [7, 8].

Considering the lack of scientific data regarding the preformulation studies of PRMS and taking into account the recent studies regarding the efficacy of vaginal tablets containing this synthetic estrogen analog and the fact that currently there is no standardized formulation on Romanian market, in this study, we set our goal in performing a complex physicochemical screening regarding the preformulation of PRMS, namely the compatibility study in solid-state of PRMS with nine pharmaceutical excipients—namely Methyl 2-hydroxyethyl cellulose (Tylose), Methyl cellulose (MethocelTM), Starch, Mannitol, Magnesium stearate, Magnesium citrate, Talc, colloidal SiO2 (Aerosil) and Polyvinylpyrrolidone K-30 (PVPK30)—using thermal analysis (TG/DTG/HF data), PXRD patterns and FTIR spectroscopy, using a methodology that was previously reported in the literature [9–16].

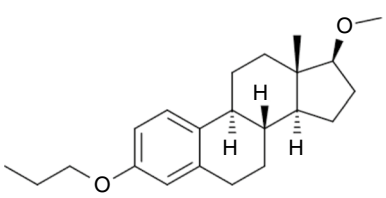

Fig. 1 Chemical structure of PRMS

Materials and methods

Reagents

Promestriene (PRMS, purity 99.5% according to USP, Suzhou Leader Chemical Co.,Ltd, Suzhou, P.R.China, CAS 39219-28-8) was a commercial product. Absolute ethanol (EtOH, purity ≥ 99.8%) was a commercial product supplied by Honeywell/Riedel-de Haën, Germany. As excipients, Methyl 2-hydroxyethyl cellulose (Tylose MH300, Sigma-Aldrich, Germany), Methyl Cellulose (Methocel® 65HG, Sigma-Aldrich, Germany), Starch (StarCap 1500, Colorcon, USA), D-Mannitol (Sigma-Aldrich, Germany), Magnesium stearate (MgSt, Mosselman, Belgium), Trimagnesium dicitrate nonahydrate (MgCit, Sigma-Aldrich, Germany), Talc (Imerys Talc, Italy), colloidal SiO_2 (Aerosil 200, Evonik Degussa, Germany) and Polyvinylpyrrolidone K-30 (PVPK30, Sigma-Aldrich, Germany) were used. All the reagents were kept sealed, in the conditions suggested by the supplier and used as received, without further purification. The producers declared that all of the compounds are suitable for use as excipients.

Sample preparation

The binary mixtures were prepared by the trituration, in an agate mortar with pestle, of equal masses of PRMS and excipient (30 mg each), for approximately 5 min. Even if in formulation the ratio between the active pharmaceutical ingredient (API) and the used excipients is considerably below 1:1, in preformulation studies, this ratio is chosen in order to facilitate the probability of observing any occurring interaction. Immediately, after preparation, the samples were sealed glass vials and kept under ambient conditions (20 ± 2 °C), in the absence of light. In parallel, a witness PRMS sample (60 mg) was dry-triturated alone for 5 min, in order to assure the same physical properties of the API as in the binary mixture (PRMS DRY TRIT), respectively, in the presence of absolute ethanol (PRMS/EtOH TRIT). These last two triturated samples were prepared in order to search of crystalline phase modification of PRMS supplied by the producer during mechanical processing of the API.

Spectroscopic investigations

FTIR spectra were recorded using a PerkinElmer SPECTRUM 100 device (PerkinElmer Applied Biosystems, Foster City, CA, USA), without preliminary preparation of the sample, using a Universal Attenuated Total Reflectance Accessory (UATR). The data were collected in 4000–650 cm^{-1} spectral range, after compression of the sample with the

pressure arm of the device, in order to get an adequate contact of it with the diamond crystal surface. Spectra were built up after a number of 64 co-acquisitions, with a resolution of 2 cm^{-1}. The background of UATR-FTIR instrument was set up before recording the spectra of each sample, and it acted as a reference for the sample measurements. The 2300–1900 cm^{-1} spectral range has no spectroscopic significance, since it represents the noise signal of the crystal. The cleaning of the optical elements of the UATR-FTIR crystal was carried out as follows: The solid sample was initially removed using a dry cotton bud and then, cleaned with cotton buds moistened with the following sequence of solvents: aqueous ethanol, absolute ethanol and acetone. Residual solvent was removed with a clean, dry cotton bud, and the next sample was placed when the spectrometer indicated that the crystal is clean (no contamination bands appear vs. reference background).

PXRD Study

The crystallinity of the analyzed samples containing PRMS was evaluated by X-ray powder diffraction (PXRD), using a Rigaku Ultima IV instrument operating at 40 kV and 40 mA. The X-ray diffraction patterns were recorded using the monochromated CuKα radiation, in continuous mode, with a scan speed of 100,000 ° min^{-1}, with a step width of 0.0500 deg, on the range 50,000–350,000 deg.

Thermal stability study

TG (thermogravimetric/mass), DTG (derivative thermogravimetric/mass derivative) and HF (heat flow) curves were simultaneously obtained in dynamic air atmosphere (100 mL min^{-1}), using open aluminum crucibles on a PerkinElmer Diamond instrument (PerkinElmer Applied Biosystems, Foster City, CA, USA). As thermal treatment regime of the samples, identical conditions were chosen for all samples, namely: non-isothermal heating at a heating rate $\beta = 10$ °C·min^{-1}, from 35 to 500 °C. For determining the thermal effects, the DTA data (in μV) were converted to HF data (in mW). All the thermoanalytical data were collected in triplicate, and the results were comparable.

Results and discussion

The aim of this study was to obtain and report, for the first time in the literature, important information regarding the stability and compatibility of PRMS as pure compound and in binary solid mixtures, with nine pharmaceutical excipients, both under ambient conditions and thermal treatment. Since recent studies reveal the good therapeutic efficacy of vaginal tablets containing PRMS after administration to patients with chronic cervicitis and HPV infection [5], as well as the complete lack of pharmaceutical formulations on the Romanian market containing PRMS, the data obtained by our group of research can represent the base in the development of new generic formulations, with a coherent and adequate selection of coformulating agents.

All the spectroscopic and diffractometric data were correlated with the thermal analysis results, leading to a complete perspective over stability of PRMS in binary mixtures, as follows.

UATR-FTIR analysis

The rational selection of UATR technique for drawing up the FTIR spectra resides both in the rapidity, precision, reproducibility and accuracy of measurements and the lack of necessity for the KBr dispersion preparation and pelleting, process that can induce API–excipient interactions, or even solid state transitions (like polymorphic transitions) due to the high applied pressure.

The FTIR spectroscopy was used in order to evaluate the possible interactions between the active substance, PRMS, and each selected excipient. The obtained spectra for each prepared binary mixture PRMS + excipient were compared to the one acquired for pure PRMS (Fig. 2). The spectral bands observed for PRMS can be easily associated with its structural characteristics. As such, the presence of the aliphatic methyl and methylene groups is revealed by the bands seen at 2956, 2931, 2865 and 2812 cm^{-1} associated with the stretching vibration of the C–H bond, as well as the ones observed at 1444 and 1379 cm^{-1}, the peaks being correlated with the asymmetric and symmetric bending vibration of the same bond. The twisting, wagging and rocking vibrations of the methylene groups are revealed by bands seen at 1297, 1280 and 739 cm^{-1}, respectively, while the in-plane bending of the methyl moiety can be associated with the peak observed at 1055 cm^{-1}. The bands seen at 1611, 1572 and 1501 cm^{-1} can be associated with the stretching vibration of the C=C bond from the aromatic ring, and the peaks observed on the spectra at 869 and 779 cm^{-1} are due to the out-of-plane bending vibration of the C–H bond from the same ring. The aliphatic ether bond determines the appearance of a band with an intense peak at 1105 cm^{-1} due to the stretching vibration of the C–O–C bond, while the vibration of the same bond type found in the aryl alkyl ether moiety is revealed by two intense bands seen at 1252 and 1026 cm^{-1} [17].

Analyzing the obtained spectra (Fig. 2) and the collected data (Table 1) for each prepared binary mixture, no interactions are suspected between the components in the case of PRMS + Tylose, PRMS + Methocel and PRMS + Starch. In these cases, the obtained spectra are almost identical to the one seen for pure PRMS, with no new bands being

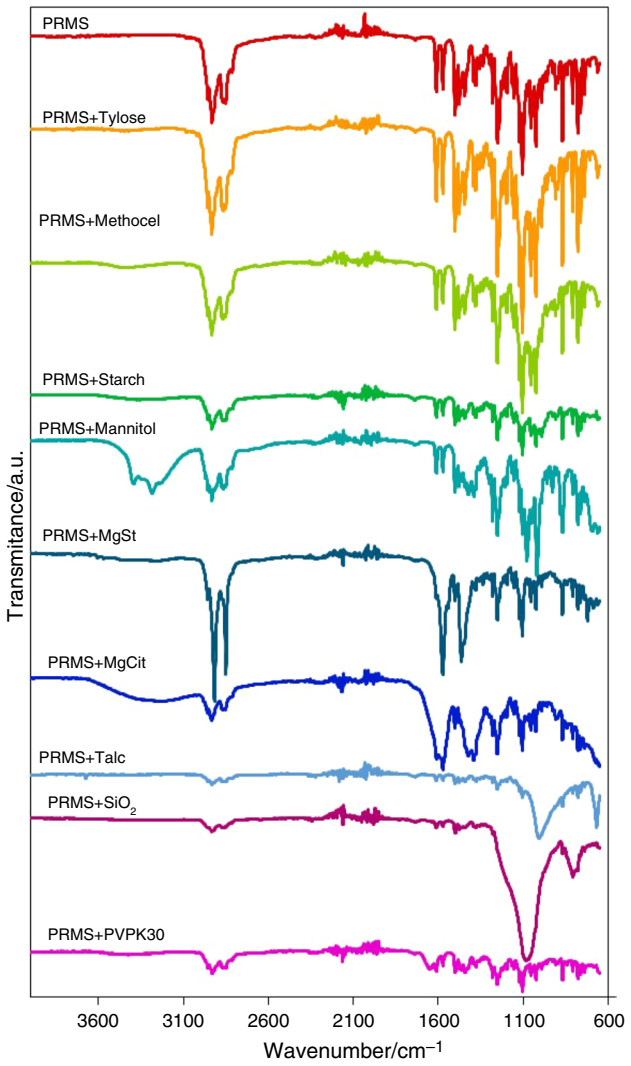

Fig. 2 UATR-FTIR spectra drawn for pure PRMS and each binary mixture PRMS + Excipient

revealed. In the case of PRMS + Mannitol, the spectrum not only contains the main bands associated with PRMS, but also the ones related to the presence of excipient, namely a broad band in the spectral range 3500–3100 cm^{-1}, with peaks at 3392 and 3281 cm^{-1} that can be associated with the stretching vibration of the O–H bonds. The presence of the excipient into the mixture is also revealed by the band seen at 1079 cm^{-1} associated with the stretching vibration of the C–O bond from the hydroxyl moieties, as well as the in-plane bending vibration of the O–H bond revealed by bands seen at 1424 and 1336 cm^{-1}.

The spectrum obtained for the mixture PRMS + MgSt is slightly modified from the one of the pure substances, PRMS, most likely due to the presence of the carboxylate anion that determines the appearance of two intense bands at 1573 and 1464 cm^{-1} associated with the asymmetric and symmetric stretching vibration. As such, the intensity of the spectral bands of PRMS is slightly diminished, although most peaks maintain their spectral position and no new bands that may indicate possible interactions can be observed.

The presence of the carboxylic and hydroxylic groups alongside the carboxylate anion in the structure of MgCit determines the modification of the spectrum of the binary mixture PRMS + MgCit when compared to that of PRMS. As such, the stretching vibration of the O–H bond from both –OH and –COOH moieties determines the appearance of a broad band at 3600–3100 cm^{-1}, while the stretching vibration of both C=O and C–O bonds from the carboxylic group and its ion can be associated with wide bands seen at 1568, 1424 and 1390 cm^{-1} that overlap with some of the bands that characterize PRMS.

The spectra obtained for PRMS + Talc and PRMS + SiO_2 are drastically altered due to the stretching vibration of the Si–O bond that determines the appearance of an intense, wide band in both cases, with peaks at 1008 cm^{-1} for the former and 1080 cm^{-1} for the latter mixture. The spectra of

Table 1 ATR-FTIR spectral bands characteristic for pure PRMS and each PRMS + excipient binary mixture

Sample	Characteristic ATR-FTIR bands/cm^{-1}		
	C–H	C=C	C–O–C
PRMS DRY TRIT	2956; 2931; 2865; 2812; 1444; 1379; 1297; 1280; 1055; 739	1611; 1572; 1501; 869; 779	1252; 1105; 1026
PRMS + Tylose	2957; 2933; 2866; 2812; 1444; 1380; 1297; 1281; 1055; 740	1612; 1572; 1502; 869; 780	1253; 1105; 1026
PRMS + Methocel	2957; 2933; 2866; 2813; 1445; 1380; 1297; 1281; 1055; 740	1612; 1572; 1502; 869; 780	1253; 1106; 1026
PRMS + Starch	2956; 2932; 2865; 2811; 1443; 1379; 1280; 1055; 740	1611; 1572; 1501; 869; 779	1252; 1105; 1025
PRMS + Mannitol	2969; 2954; 2932; 2865; 2812; 1443; 1380; 1298; 1281; 1056; 739	1611; 1572; 1501; 868; 780	1253; 1105; 1020
PRMS + MgSt	2856; 2917; 2850; 1281; 1054; 739; 723	1610; 1542; 1502; 868; 780	1254; 1106; 1026
PRMS + MgCit	2957; 2933; 2866; 2813; 1281; 1056; 739	1612; 1501; 868; 780	1254; 1105; 1026
PRMS + Talc	2955; 2930; 2861; 1379; 1280; 739	1611; 1572; 1500; 868; 779	1252; 1105; 1025
PRMS + SiO_2	2958; 2931; 2869; 1379; 1280; 739	1610; 1572; 1501; 868; 780	1251; 1103; 1024
PRMS + PVPK30	2956; 2931; 2863; 2811; 1280; 1055; 739	1610; 1572; 1501; 868; 779	1257; 1104; 1025

the PRMS + PVPK30 mixture revealed the presence of a band at 1654 cm^{-1} that could be associated with the stretching vibration of the C=O bond present in the structure of the excipient, but also the characteristic bands of PRMS. As a conclusion, no interactions are suspected in none of the analyzed binary mixtures.

PXRD pattern analysis

PRMS was investigated by PXRD tool as pure API, provided by the supplier, without being mechanically processed, but as well after two trituration procedures in an agate mortar with a pestle, in the same conditions as the analyzed binary mixtures: (1) dry trituration, i.e., the kneading of pure PRMS and (2) wet trituration, the kneading of PRMS in the presence of few drops of absolute ethanol, until the solvent completely evaporates. After these procedures, the samples were placed in oven at 35 °C, for 24 h, and then, the PXRD patterns were recorded, as seen in Fig. 3.

The analysis of PXRD patterns for PRMS in the form provided by the supplier greatly differs from the one recorded after dry and wet trituration of the API. The characteristic peaks are presented in Table 2, suggesting that different crystalline forms of PRMS exist, and this polymorphic transition takes place easy, just by simple trituration of PRMS, in the presence or absence of an added solvent. In the case of mechanical processed samples, PXRD patterns also suggest that trituration determines the decrease in the average crystallite size, since the broadening of the PXRD peaks takes place. As it can be seen in Fig. 4 and Table 2, the peak positions of the diffraction signals of PRMS are unchanged in the binary mixtures with excipients, suggesting the lack of incompatibility between the components. However, it is also obvious that the diffraction peaks of the micronized samples (pure API and all binary mixtures) are much broader than those of the PRMS supplied by the producer, suggesting that the crystallite size is reduced by mechanical processing. The finding suggested by this instrumental technique is in good agreement with the UATR-FTIR spectroscopic data, i.e., that under ambient conditions, there are no chemical interactions that occur between the components of binary mixtures.

Thermal stability study

In order to get a complete perspective over compatibility/incompatibility of PRMS with selected excipients, the effect of thermal stress on all samples was investigated, initially for pure API and later on binary mixtures.

The thermoanalytical curves obtained at $\beta = 10$ °C·min^{-1} for PRMS are presented in Fig. 5. PRMS shows a good thermal stability (up to 173 °C), assured by the presence of the steroid moiety. In the temperature range 35–173 °C, no mass loss occurs. Above 173 °C, the decomposition of

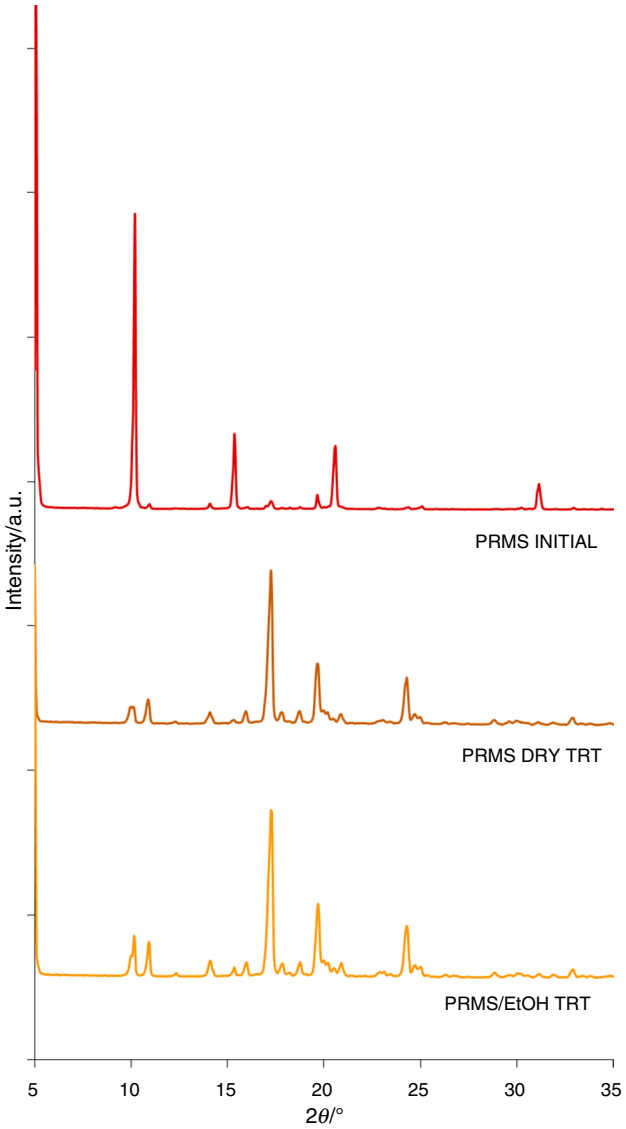

Fig. 3 Comparative PXRD patterns recorded for PRMS: as provided by the supplier (PRMS INITIAL), the dry trituration product (PRMS DRY TRIT) and the kneaded product of PRMS with absolute EtOH (PRMS/EtOH TRIT)

PRMS begins, with a residual mass at 500 °C of 1.40% ($\Delta m_{total} = 98.60\%$). In this temperature range, the rapid mass loss takes place between 211 and 331 °C ($\Delta m = 95.47\%$). This single-step process of mass loss is also evidenced by the DTG curve that presents one well-individualized process, in the 174–347 °C interval, with a maximum at 312 °C. The HF curve reveals the presence of three main processes that are associated with heat change during the phase transitions, as follows: The first endothermic process that takes place in 59–80 °C range (HF_{peakI} at 66 °C) is represented by the solid–liquid phase transitions, the value being in good agreement with the literature data [4, 18], followed by a broad exothermic process, associated with mass loss due

Table 2 PXRD pattern results (as peaks) for the analyzed samples containing PRMS

Sample	PXRD peaks (2θ (degrees))
PRMS INITIAL	10.20; 15.35; 19.65; 20.55; 31.05
PRMS DRY TRIT	10.20; 10.85; 14.10; 15.25; 15.85; 17.25; 17.75; 18.65; 19.65; 20.80; 24.25; 32.80
PRMS/EtOH TRIT	10.15; 10.85; 14.10; 15.25; 15.85; 17.25; 17.75; 18.65; 19.65; 20.80; 24.25; 32.80
PRMS + Tylose	10.15; 10.85; 14.10; 15.25; 15.85; 17.25; 17.75; 18.65; 19.65; 20.80; 24.25; 32.80
PRMS + Methocel	10.20; 10.85; 14.15; 15.25; 15.85; 17.25; 17.75; 18.65; 19.60; 20.85; 24.25; 32.80
PRMS + Starch	10.20; 10.85; 14.10; 15.25; 15.85; 17.20; 17.75; 18.65; 19.65; 20.80; 24.25; 32.85
PRMS + Mannitol	10.20; 10.85; 14.10; 14.40*; 15.25; 15.35*; 15.85; 16.55*; 17.25; 17.75; 18.65; 19.65; 20.20*; 20.80; 24.25; 25.65*; 29.25*; 32.80; 33.30*
PRMS + MgSt	5.05*; 8.65*; 10.15; 10.85; 14.10; 15.25; 15.85; 17.25; 17.75; 18.65; 19.65; 20.80; 21.55*; 22.35*; 24.25; 32.80
PRMS + MgCit	8.80*; 10.15; 10.85; 11.20*; 14.10; 15.25; 15.85; 17.25; 17.75; 18.65; 19.65; 20.80; 24.25; 32.80
PRMS + Talc	9.30*; 10.15; 10.85; 14.10; 15.25; 15.85; 17.25; 17.75; 18.65; 19.65; 20.80; 24.25; 28.50*; 32.80
PRMS + SiO2	10.15; 10.85; 14.10; 15.25; 15.85; 17.25; 17.75; 18.65; 19.65; 20.80; 24.25
PRMS + PVPK30	10.20; 10.85; 14.10; 15.25; 15.85; 17.25; 17.75; 18.65; 19.65; 20.80; 24.25; 32.85

*Peaks corresponding to excipient

to thermooxidations in the temperature range 80–304 °C (HF_{peakII} at 277 °C) and lastly by a new endothermic process in the 304–336 °C temperature range ($HF_{peakIII}$ at 319 °C). This latter endothermic process may suggest the superimposition of the decomposition with the evaporation of PRMS, but it cannot be confirmed since no literature data were found regarding the boiling point of this API, except a prediction (436.8 ± 45.0 °C) [4], which is far from the observed values and is not confirmed by our experimental data.

At temperatures above 336 °C, the thermal effects are negligible, as the char formed above this temperature is no longer susceptible to thermolysis, the corresponding mass loss being insignificant ($\Delta m = 1.62\%$).

Figure 6 presents the thermoanalytical curves obtained for pure PRMS and the analyzed binary mixtures with excipients. The analysis of PRMS + Tylose mixture reveals the first mass loss due to dehydration (loss of absorbed water) in the range 35–57 °C (corresponding mass loss $\Delta m = 1.64\%$), process also revealed by the DTG curve (range 35–56 °C) and the HF curve (between 35 and 51 °C, peak at 42 °C). In the temperature interval 57–163 °C, the mass is constant, corresponding to the anhydrous mixture of API and excipient, initially in solid state (according to the HF curve in the 51–60 °C interval) and later containing melted PRMS (HF endothermic event in 60–73 °C range, peak at 65 °C). Since the melting process of PRMS is unaltered by the presence of Tylose, no interactions are suspected in this binary mixture. However, the decomposition of the mixture begins at 163 °C, as suggested by all thermoanalytical curves: In the temperature interval 163–376 °C, the mass loss is considerable ($\Delta m = 84.35\%$), and the DTG curve suggesting a two-step process, with peaks at 274 °C and 328 °C, also confirmed by the HF curve by two exothermic processes: the first taking place between 164–220 °C (peak at 194 °C) and the second in the 220–374 °C (peak at 323 °C). At temperatures over 376 °C and up to 500 °C, the degradative process is intense due to thermooxidation of organic skeletons of both PRMS and Tylose ($\Delta m = 13.3\%$, DTG_{max} at 460 °C, HF_{max} at 461 °C).

Methocel is also compatible with PRMS, since the mixture has a good thermal stability up to 144 °C. Superficial adsorbed water is released from the physical mixture in the temperature range 35–52 °C ($\Delta m = 1.21\%$). At temperatures inferior to 144 °C, the HF curve reveals the melting of PRMS (onset of melting occurring at 59 °C, peak at 66 °C and offset at 78 °C). Between 144 °C and 393 °C, a multistep degradation occurs, as suggested by the DTG curve, by maximums at 265, 291 and 346 °C; in this range, exothermic thermolysis occurs between 148 and 247 °C (HF_{max} at 204 °C and 241 °C) and 273–388 °C (HF_{max} at 324 °C and 341 °C), with a partial mass loss $\Delta m = 85.79\%$. In the last stage of degradation, the intense exothermic thermolysis that occurs between 388–500 °C led to a final insignificant residual mass of 2.61%.

The thermoanalythical profile of the PRMS + Starch mixture shows a small mass loss between 35 and 67 °C ($\Delta m = 2.21\%$) due to the dehydration of the polysaccharidic excipient, then the mass remains constant up to 182 °C. Between 182 °C and 386 °C, a two-step decomposition process takes place (two well-individualized process on the DTG curve, with DTG_{peaks} at 287 °C and 314 °C), with a considerable partial mass loss ($\Delta m = 85.7\%$) and, later, between 386 and 500 °C, with DTG_{peak} at 496 °C and total mass loss $\Delta m = 99.48\%$. The HF curve suggests the compatibility between PRMS and Starch, since the melting process of the API takes place in the same interval as seen for the pure derivative (60–80 °C).

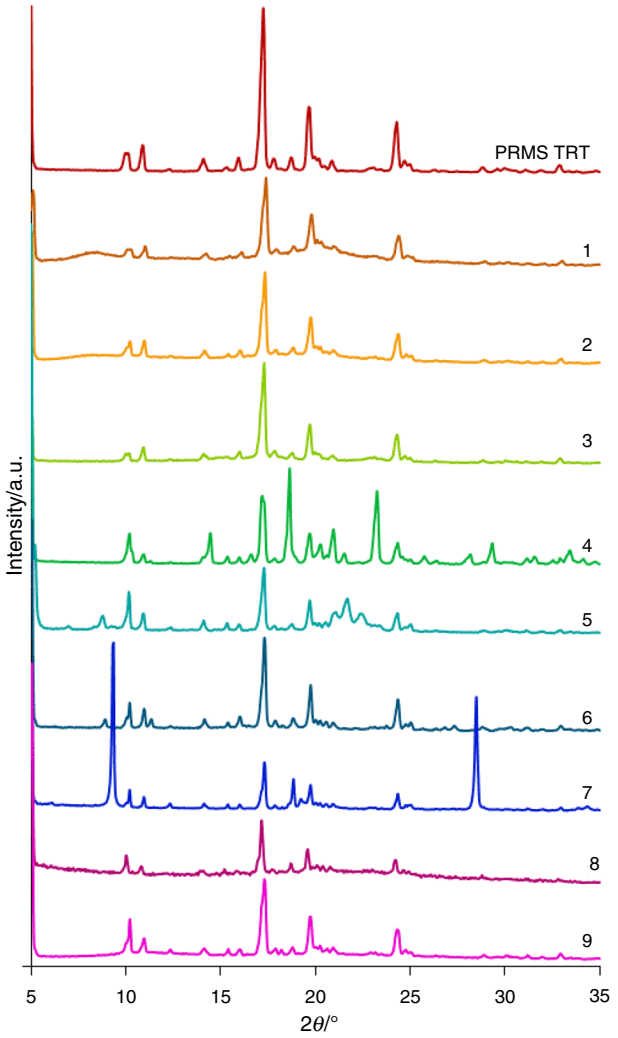

Fig. 4 Comparative PXRD patterns recorded for PRMS DRY TRIT (1) and each binary mixture, as follows: (1) PRMS + Tylose; (2) PRMS + Methocel; (3) PRMS + Starch; (4) PRMS + Mannitol; (5) PRMS + MgSt; (6) PRMS + MgCit; (7) PRMS + Talc; (8) PRMS + SiO_2 and (9) PRMS + PVPK30

PRMS is also compatible with Mannitol, since the thermoanalytical curves of the mixture reveal a good thermal stability up to 183 °C, with no mass loss but with two phase transitions suggested by the HF curve: melting of PRMS (61–77 °C, peak at 67 °C) and melting of mannitol (162–181 °C, peak at 167 °C), in agreement with the literature [19]. It is interesting to notice that the compatibility of these two compounds is observed even in liquid state, since no melting interval alliteration is observed. The main mass loss (95.24%) occurs between 183 and 360 °C by the contribution of three different processes, as suggested by the DTG curve, with peaks at 286, 322 and 341 °C. At 500 °C, the mass loss is complete ($\Delta m = 99.21\%$).

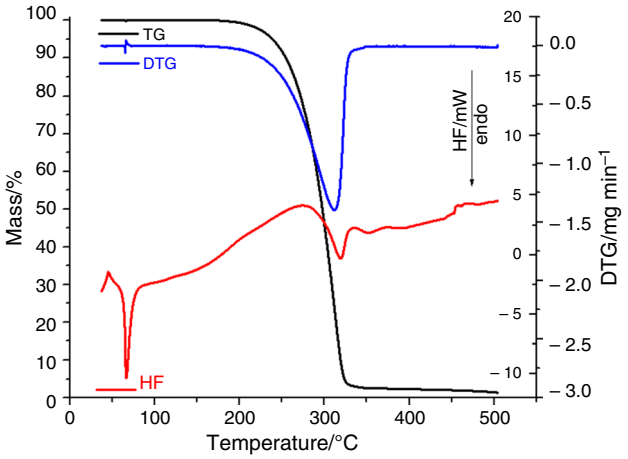

Fig. 5 TG/DTG/HF thermoanalytical curves obtained during thermal treatment in dynamic air atmosphere for PRMS at $\beta = 10$ °C·min^{-1}

The thermoanalytical curves corresponding to PRMS + MgSt mixture indicate a complex pathway of decomposition, since incompatibility is observed at temperatures higher than 150 °C, as the disappearance of HF processes that occur for pure PRMS in the temperature range 80–336 °C. However, by the correlation of thermal data with the spectroscopic ones, it is clearly suggested that between 35 and 76 °C, and the compounds are compatible (HFpeak for PRMS melting in binary mixture is observed at 67 °C). At 500 °C, the residual mass is 5.36% due to impossibility of complete oxidation of Mg^{2+} containing char.

MgCit is compatible with PRMS. Between 35 and 71 °C, the dehydration of the excipient occurs, and the TG curve showing no mass loss up to 96 °C. The melting of API takes place in the range 47–80 °C (HF_{max} at 66 °C), as seen on the HF curve. As the temperature increases, a similar thermoanalytical profile is observed for the binary mixture as the one seen for pure PRMS, suggesting the lack of interaction between the components even at high temperatures. The mass loss is rapid between 122 and 294 °C, being 55.67%. As observed for MgSt, in this case also, the residual mass at 500 °C is considerable (28.86%), due to the resilience of magnesium containing chars.

For the PRMS + Talc mixture, the thermal stability is good (up to 176 °C) and the only observed thermal event is the melting of PRMS (peak at 66 °C). The mass loss takes place in a single-step process, between 176 and 291 °C, with an associate $\Delta m = 48.87\%$ and identical peaks on DTG and HF curves (maximum rate of mass loss at 276 °C, due to an exothermic event). Between 291 and 500 °C, the mass loss is $\Delta m = 1.55\%$, so the residual mass is 49.70%, corresponding to the mass of the remaining inert excipient from the 1:1 (mass/mass) mixture. As a conclusion to the results, no interactions take place between PRMS and Talc.

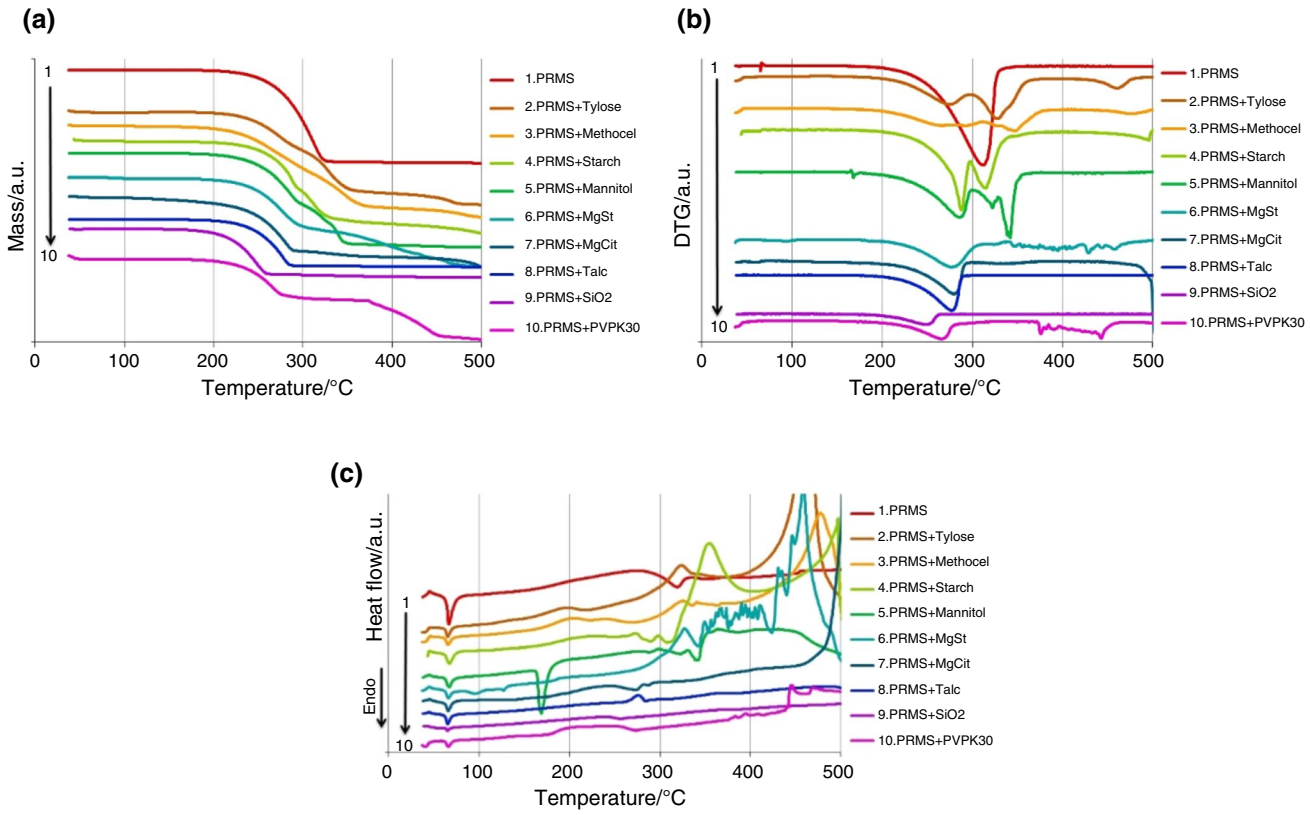

Fig. 6 TG/DTG/HF thermoanalytical curves obtained for PRMS and binary mixtures with excipients: **a** Mass versus temperature (TG curves); **b** Mass derivative vs. temperature (DTG curves) and **c** Heat flow versus temperature (HF curves)

A similar behavior is observed for the PRMS + SiO_2 mixture: No mass loss occurs up to 138 °C, then the decomposition begins (DTG_{peak} at 247 °C, offset at 271 °C, corresponding $\Delta m = 47.98\%$). The HF profile is similar to the one observed for pure PRMS (melting at 66 °C), suggesting the compatibility between PRMS and SiO_2 even at high temperatures. Residual mass is, in this case too, half of the mass of initial sample (49.56%), due to the thermal inertia of colloidal silica.

The PRMS + PVPK30 mixture displays a complex decomposition process, occurring in several steps, with the formation of at least two stable intermediates, in the temperature ranges 59–169 °C and 320–374 °C. At temperatures below 277 °C, HF curve is very similar to the one of PRMS, revealing the melting in the 62–76 °C interval, with a peak seen at 66 °C. Three main steps of mass loss are observed: The first is the initial release of adsorbed water under 48 °C (endotherm process with $\Delta m = 3.27\%$, peak at 41 °C); the second takes place between 169 and 320 °C (DTG_{peak} at 265 °C, exothermic decomposition with $\Delta m = 42.13\%$), and the third is represented by multiple peaks (main at 376 °C and 442 °C according to DTG curve, exothermic oxidations) in 374–500 °C interval ($\Delta m = 41.02\%$).

Surprisingly, none of the investigated excipients showed interactions with PRMS, suggesting that newly developed formulations can be prepared taking into account these excipients, in the development of new tablets. The lack of interaction between PRMS and these varied structure excipients can be explained by the presence of chemically inert moieties, namely the etheric 3-propoxy and -17β-methoxy ones.

Conclusions

In this paper, ten samples containing PRMS were investigated, namely the pure pharmaceutical compound and nine binary mixtures with pharmaceutical excipients commonly used in solid formulations. The necessity of a study which addresses this topic is represented by the fact that the physicochemical screening of promestriene is not reported in the literature, up to the date. The study revealed that PRMS is compatible with all selected excipients, namely Methyl 2-hydroxyethyl cellulose (Tylose), Methyl Cellulose (Methocel™), Starch, Mannitol, Magnesium stearate, Magnesium citrate, Talc, colloidal SiO_2 (Aerosil) and Polyvinylpyrrolidone K-30 (PVPK30), under ambient conditions, as

suggested by FTIR spectroscopy and PXRD patterns, as well as under thermal stress, as suggested by the thermoanalytical results. The lack of interaction between PRMS and the selected excipients can be explained by the fact that this synthetic estrogen analog of estradiol possess as functional moieties solely two etheric groups (i.e., 3-propoxy and -17β-methoxy ones), with decreased chemical reactivity. The find outs reported in this paper can serve as starting point in the adequate selection of ingredients for magistral preparations, with increased stability and bioavailability.

Author contributions All authors contributed to the design and analysis of the study. All authors participated in writing the manuscript. All authors read and approved the final manuscript.

Funding This research was funded by UEFISCDI, PN-III-P1-1.1-TE-2016-1165 project (RECOTHER) to Adriana Ledeți, Ionuț Ledeți, Denisa Cîrcioban and Carmen Tomoroga.

References

1. Santos I, Clissold S. Urogenital disorders associated with oestrogen deficiency: the role of promestriene as topical oestrogen therapy. Gynecol Endocrinol. 2010;26(9):644–51.
2. Almodovar AJO, Litherland SA, Courtneidge S, Decker DA. Promestriene effects on estrogen-sensitive breast cancer cell proliferation in vitro. Cancer Res. 2013. https://doi.org/10.1158/0008-5472.SABCS13-P5-05-07.
3. Del Pup L, Di Francia R, Cavaliere C, Facchini G, Giorda G, De Paoli P, Berretta M. Promestriene, a specific topic estrogen. Review of 40 years of vaginal atrophy treatment: is it safe even in cancer patients? Anticancer Drugs. 2013;24(10):989–98.
4. Promestriene on Chemicalbook.com. https://www.chemicalbook.com/ChemicalProductProperty_EN_CB5266119.htm. Accessed 26 Oct 2022.
5. Chen X, Guo H. Comparison of chlorquinaldol-promestriene vaginal tablets and opin suppositories effect on inflammatory factors and immune function in chronic HPV cervicitis. J Coll Physicians Surg Pak. 2019;29(2):115–8.
6. Promestriene on Web of Science Clarivate Analytics. https://www-webofscience-com.am.e-nformation.ro/wos/woscc/summary/4c572334-aebf-4b4f-aef9-4ad8fc1e42ad-58f8dcde/relevance/1. Accessed 26 Oct 2022.
7. Romania's Ministry of Health—Missing Drugs Section. http://medicamentelipsa.ms.ro/?page=174. Accessed 10 Oct 2019.
8. List of Romanian Drugs for Human Use. https://www.anm.ro/nomenclator/medicamente. Accessed 22 Oct 2022.
9. Ledeti I, Vlase G, Vlase T, Suta L-M, Todea A, Fulias A. Selection of solid-state excipients for simvastatin dosage forms through thermal and nonthermal techniques. J Therm Anal Calorim. 2015;121(3):1093–102.
10. Ledeti I, Bolintineanu S, Vlase G, Circioban D, Dehelean C, Suta LM, Caunii A, Ledeti A, Vlase T, Murariu M. Evaluation of solid-state thermal stability of donepezil in binary mixtures with excipients using instrumental techniques. J Therm Anal Calorim. 2017;130(1):425–31.
11. Ledeţi I, Budiul M, Matusz P, et al. Preformulation studies for nortriptyline: solid-state compatibility with pharmaceutical excipients. J Therm Anal Calorim. 2018;131(1):191–9.
12. Ledeti I, Pusztai AM, Muresan CM, et al. Study of solid-state degradation of prochlorperazine and promethazine. J Therm Anal Calorim. 2018;134(1):731–40.
13. Trandafirescu C, Soica C, Ledeti A, Borcan F, Suta L-M, Murariu M, Dehelean C, Ionescu D, Ledeti I. Preformulation studies for albendazole: a DSC and FTIR analysis of binary mixtures with excipients. Rev Chim. 2016;67(3):463–7.
14. Ledeti I, Bercean V, Alexa A, Soica C, Suta L-M, Dehelean C, Trandafirescu C, Muntean D, Licker M, Fulias A. Preparation and antibacterial properties of substituted 1,2,4-triazoles. J Chem. 2015. https://doi.org/10.1155/2015/879343.
15. Trandafirescu C, Gyeresi A, Szabadai Z, Kata M, Aigner Z. Solid-state characterization of bifonazole-beta-cyclodextrin binary systems. Note I Farmacia. 2014;62(3):513–23.
16. Ledeţi A, Vlase G, Vlase T, Bercean V, Murariu MS, Ledeţi I, Şuta LM. Solid-state preformulation studies of amiodarone hydrochloride. J Therm Anal Calorim. 2016;126(1):181–7.
17. Silverstein RM, Webster FX, Kiemle DJ. Spectrometric identification of organic compounds. Spectrom Identif Org Compd. 2005. https://doi.org/10.1016/0022-2860(76)87024-X.
18. Sittig M. Pharmaceutical manufacturing encyclopedia, vol. 4. 3rd ed. Norwich: William Andrew Publishing; 2007. p. 270–2.
19. Gombás Á, Szabó-Révész P, Regdon G, Erös I. Study of thermal behaviour of sugar alcohols. J Therm Anal Calorim. 2003;73(2):615–21.